Title

Needle-Electrode-Based Electromechanical Reshaping of Rabbit Septal Cartilage: A Systematic Evaluation

Journal

IEEE Transactions on Biomedical Engineering, 58(8)

ISSN

0018-9294

Authors

Wu, Edward C

Protsenko, Dmitriy E

Khan, Adam Z

et al.

Publication Date

2011-08-01

DOI

10.1109/tbme.2011.2157155

Published in final edited form as:
IEEE Trans Biomed Eng. 2011 August ; 58(8): . doi:10.1109/TBME.2011.2157155.

Needle-Electrode-Based Electromechanical Reshaping of Rabbit Septal Cartilage: A Systematic Evaluation

Edward C. Wu,
Beckman Laser Institute and Medical Clinic, Irvine, CA 92612 USA wuec@uci.edu.

Dmitriy E. Protsenko,
Beckman Laser Institute and Medical Clinic, Irvine, CA 92612 USA dprotsen@uci.edu

Adam Z. Khan,
Beckman Laser Institute and Medical Clinic, Irvine, CA 92612 USA. He is now with the Department of Bioengineering, California Institute of Technology, Pasadena, CA 91125 USA adamkhan@caltech.edu

Sterling Dubin,
Beckman Laser Institute and Medical Clinic, Irvine, CA 92612 USA. He is now with the George Washington University School of Medicine, Washington, DC 20037 USA sterling.dubin@gmail.com

Koohyar Karimi, and
Beckman Laser Institute and Medical Clinic, Irvine, CA 92612 USA and is now with the Loma Linda University School of Dentistry, Loma Linda, CA 92350 USA fluxed04@yahoo.com

Brian J. F. Wong
Beckman Laser Institute and Medical Clinic, Irvine, CA 92612 USA bjwong@uci.edu

Abstract

Electromechanical reshaping (EMR) provides a means of producing shape change in the cartilage by initiating oxidation–reduction reactions in mechanically deformed specimens. This paper evaluates the effect of voltage and application time on specimen shape change using needle electrodes. Rabbit septal cartilage specimens (20 mm × 8 mm × 1 mm, n = 200) were bent 90° in a precision-machined plastic jig. Optimal electrode placement and the range of applied voltages were estimated using numerical modeling of the initial electric field within the cartilage sample. A geometric configuration of three platinum needle electrodes 2 mm apart from each other and inserted 6 mm from the bend axis on opposite ends was selected. One row of electrodes served as the anode and the other as the cathode. Constant voltage was applied at 1, 2, 4, 6, and 8 V for 1, 2, and 4 min, followed by rehydration in phosphate buffered saline. Samples were then removed from the jig and bend angle was measured. In accordance with previous studies, bend angle increased with increasing voltage and application time. Below a voltage threshold of 4 V, 4 min, no clinically significant reshaping was observed. The maximum bend angle obtained was 35.7 ± 1.7° at 8 V, 4 min.

Correspondence to: Brian J. F. Wong.

Index Terms

Electromechanical cartilage reshaping; needle-electrode geometry

I. Introduction

Cartilage forms the framework for the upper airway and the structural aesthetic features of the face, and reshaping this tissue is necessary in reconstructive and aesthetic surgery in the head, neck, and upper airway. Over the past two decades, new techniques involving lasers [1]–[5], radiofrequency devices [6], and enzymatic digestion [7] have been developed to change the shape of cartilage tissue and perform surgery without scalpels, incisions, or sutures. Potential applications include, correcting congenital malformations of the external ear (otoplasty), improving the patency of the nasal airway (septoplasty), altering the shape of the nose (rhinoplasty), as well as correcting complex injuries of the larynx and trachea. Traditional surgical techniques aimed at altering shape generally require incising and/or suturing cartilage to release or balance the intrinsic forces that resist sustained deformation [8]–[10].

Thermal methods aimed at achieving shape change in the cartilage have primarily used lasers to heat tissue focally as they provide precise control over the spatial and temporal evolution of heat [1]–[5], though radiofrequency sources have been explored as well [6]. However, “thermoforming” may lead to tissue injury, and there is a tradeoff between shape change and cell damage. An alternative to thermoforming methods relies on *in situ* redox reactions in the tissue matrix of mechanical deformed cartilage specimens using low-level dc voltages generating currents in the milliampere range [11]–[13]. This electromechanical reshaping (EMR) process exploits the properties of the cartilage as a charged polymer hydrogel. Cartilage tissue is first deformed or straightened into the desired shape and electrodes are then positioned in the vicinity of the internal stress concentrations. A constant voltage is applied to the electrodes initiating a series of redox reactions at the tissue–electrode interfaces. We have demonstrated that these electrochemical reactions, while complex, act synergistically to locally alter the chemical composition of cartilage resulting in relaxation of internal stress and subsequent stable shape change [12], [13]. Compared to thermoforming, EMR at appropriate voltage levels produces a negligible temperature elevation suggesting that the shape change occurs without any contribution from resistive heating [13].

Previously, EMR has been studied using large, flat surface electrodes [12], [13] and, more recently, with platinum needle electrodes [11], [14]. The degree of shape change increases with both voltage and application time using both electrode types [11]–[14]. However, performing EMR with the surface electrodes sandwiching both sides of a cartilage sample produces a diffuse region of chemical injury along both tissue– electrode interfaces that increases in depth with voltage and application time [15]. Likewise, the use of surface electrodes requires wide skin incisions for electrode introduction, which partially negates the impact of EMR as a minimally invasive alternative to traditional “cut and suture” surgical techniques; though such an approach may have applications in other operations such as in

total auricular reconstruction. In contrast, needle-electrode-based EMR overcomes these limitations, as fine-gauge needles can be inserted into cartilage through the skin or mucosa and the extent of tissue injury can be spatially limited based upon prudent electrode placement and partial electrical insulation of the needles. In addition, the geometric configuration and location of the needle electrodes can be customized, thereby permitting construction of an electrode configuration that will conform with the geometry of potential shape change and internal stress distributions.

Manuel *et al.* demonstrated the feasibility of sustained deformation of a flat cartilage specimen using needle-electrode-based EMR [14]. Eight needle electrodes were arranged into three parallel arrays to reshape a flat cartilage specimen [11], [14]. The central electrode array was inserted along the bend axis and two lateral flanking arrays were positioned 3 mm from the bend. While this configuration produced adequate shape change, such an electrode configuration is disadvantageous in that the central needle array penetrates the bend axis, which can contribute to bending as perforation locally alters the mechanical integrity of the specimen in tandem with EMR. In this study, we used two parallel electrode arrays flanking the bend axis rabbit nasal septal cartilage specimens bent 90°. This study aims to: 1) numerically estimate the initial electric field surrounding needle electrodes inserted into a cartilage specimen, and use this model to estimate the voltage levels needed to produce clinically significant shape change with minimal tissue injury; 2) systematically evaluate the dependence of the shape change on voltage and application time; and 3) identify voltage and application time thresholds for the onset and plateau region for the EMR effect.

II. Methods

A. Tissue Specimens

Tissue harvesting and preparation methods were previously described and are only briefly reviewed here [11]. Rabbit nasal septal cartilage specimens were extracted from freshly euthanized rabbits (<24 h) obtained from a local abattoir. Each nasal septal cartilage yielded a single tissue specimen, which was then cut (20 mm × 8 mm× 1 mm) and maintained in a shallow pool of phosphate buffered saline (PBS, pH 7.4) at ambient temperature. EMR was performed immediately after extraction and sample preparation. A total of 200 specimens were evaluated.

B. Reshaping, Transferred Charge, and Bend-Angle Measurement

Electrode configuration consisted of two arrays of three needle electrodes [11]. Platinum needle electrodes (0.3 mm diameter, Grass Technologies, West Warwick, RI) were chosen for their high standard potential and hence minimal risk of electrode oxidation [11].Custom, precision-machined reshaping jigs were designed to bend the cartilage samples into right angles (see Fig. 1). Each specimen was placed into the jig and electrodes were inserted through precision-drilled ports into the cartilage specimen. The ports allowed arrays to be positioned 3 mm from either side of the bend axis with the electrodes separated 2 mm from each other within arrays. The electrodes are connected to a dc power supply (Model PPS-2322, Amrel, Arcadia, CA), with one array designated as the anode and the other as the cathode.

To study the dependence of shape change on voltage and application time guided by results from our numerical model (see in the following), electric voltages of 1, 2, 4, 6, and 8 V as well as a negative control (0 V) were applied for 1, 2, and 4 min [11]. Electric current was monitored during voltage application, and the total charge transferred in the EMR circuit was calculated using custom-programmed software (LabView, Austin, TX). Following voltage applications, the needle electrodes were removed, and the jig containing the specimen was rehydrated in PBS for 15 min. The specimen was then removed from the jig and photographed twice with two views: as is placed and with the specimen flipped along its width to minimize the impact of both parallax and specimen nonuniformity. Bend angles are measured using ImageJ (National Institute of Health, Bethesda, MD) and differences between parameters analyzed using unpaired *t*-tests.

C. Numerical Estimation of the Electric Field

The potential voltage, application times, and electrode geometry (both spatially and with respect to polarity) combinations for EMR are innumerable, and we attempted to enhance a trial-and-error empirical approach with a rudimentary attempt at modeling. We assumed that cartilage electric conductivity is homogeneous and constant and estimated the steady-state electric field in cartilage in the moment immediately in the beginning of EMR. This estimation is a useful zero-order approximation for comparison of various electrode geometries. In theory, generation of identical electric field distributions using different voltage and needle-electrode placement geometries should lead to a similar degree of shape change. The strength of the electric field in the vicinity of tissue–electrode interfaces is related to the rate of electrochemical reactions. In turn, these redox reactions produce a permanent mechanical effect which likely occurs at the expense of tissue viability. We can grossly estimate the correlation of the electric field strength with shape change and tissue viability from our previous studies using flat surface electrodes [see Fig. 2(a) and (b)] [12], [13]. Then, finding the value of the electric field that result in acceptable shape change and viability, we can attempt to better select voltage and electrode geometry for needle-based EMR using numerical simulation of electric field distribution between needle electrodes [see Fig. 3(a) and (b)].

We calculated the electric field as a function of applied voltage, number of electrodes, and geometric configuration of the electrode arrays using a finite element modeling software package (COMSOL Multiphysics, Burlington, MA). The grid resolution was better than 5 μ m. Asurface-electrode EMR was modeled for a 15 mm × 5 mm × 1 mm cartilage specimen bended into a semicircle between concave and convex semicylindrical electrodes [see Fig. 2(a) and (b)]. Application of voltages from 2 to 6 V was simulated. A needle-electrode EMR was modeled for a 20 mm × 8 mm × 1 mm specimen bent 90° and for two symmetrical arrays of three needle electrodes 0.3mm in diameter [see Fig. 3(a) and (b)]. The arrays positioned from 2 to 12 mm from the bend axis and voltages from 2 to 12 V were modeled. The choice of electrode geometry was based on practical consideration governed by surgeon preferences (e.g., how closely surgeons can place electrodes adjacent to one another).

The data from experiments with surface-electrode EMR suggest that there is an association between the initial electric field intensity within the cartilage, steady-state tissue shape

change, and acute cell viability. In these experiments, we have determined that for applied voltages varying from 2 to 6 V (cartilage tissue thicknesses of 2 mm, one or more minutes of voltage application), reshaping degree increases from 20% to 80% while the fraction of live chondrocytes decreases from 80% to 20% [15]. A tissue injury range between 20% and 80% is tolerable in many facial cartilage applications, and this degree of tissue injury is common using conventional surgical techniques. For example, when morselization is used to reshape cartilage, tissue injury may exceed 40% to 75% [16], [17]. Numerical estimates of the electric field produced over this voltage range varied from 2.0 ±0.2 to 6.0 ±0.6 kV/cm, and, while limited, electric fields in the range of 1.8 to 6.6 kV/cm were chosen for evaluation in this study [see Fig. 2(c)] under the assumption that they will produce clinically significant reshaping without tissue injury exceeding 80% for a voltage application time of 2 min.

Using this rough assumption on electric field strength regarding the relationship between the electrical field and cell viability, the initial electric field produced by the needle-electrode system in the cartilage specimen secured in a 90° bending jig was simulated (see Fig. 3). To comply with the estimated range for the electric field and select optimal electric voltage and electrode geometry two approximate criteria were used: 1) electric field at a distance from the center of any electrode $r0.5$ should be less than 6.6 kV/cm and 2) average electric field within the bend region defined as cartilage region extending in any direction by no more than 1 mm from the bend axis should be higher than 1.8 kV/cm. Based upon results from the simulation, the electrode geometry (arrays at 6 mm distance from the bend) and voltage range (1–8 V) which most closely satisfies the used criteria for the electric field near the electrodes and within the bent region of the specimen [see Fig. 3(c)–(d)] was selected for the experimental evaluation.

III. Results

The average bend angle for electrode arrays positioned 6 mm from the bend apex for each voltage and application time combination was measured; differences were clearly observed (see Fig. 4). Unpaired *t*-tests ($\alpha < 0.05$) were used to determine statistically significant changes in the bend angle as a function of applied voltage when compared to control. Fig. 5 displays the bend angle as a function of voltage. A bend angle of 28.5 ± 1.3°, statistically exceeding the values obtained in control experiments (no voltage applied to needle electrodes inserted into tissue), was not observed below a threshold voltage and application time combination of 4 V and 4 min. The average bend angles at all voltage–time combinations below this threshold dosimetry value were statistically identical to controls (average value of 18.7 ± 2.1°) except at the 1 min control (average value of 13.8 ± 1.5°). Statistically relevant increases in bend angle were observed with voltage and application time above either threshold value. The maximum shape change achieved was a bend angle of 35.7 ± 1.7°, corresponding to the 8 V and 4 min combination.

Fig. 6 demonstrates the typical evolution of electric current in the EMR circuit measured during application of 0, 2, 4 and 8 V for 2 min. Negative (relative to chosen polarity of the electrodes) electric current was observed in all experiments performed at or below 2 V. Increasing applied voltage resulted in a corresponding increase in peak electric current.

Maximum electric current did not exceed 80 mA for any voltage and application time pair. No parameter set produced temperature elevations above 10 °C.

IV. Discussion

EMR of facial cartilages using percutaneous or transmucosal needles may have the potential to replace traditional suture and scalpel surgery in select facial operations. Though precise mechanisms of EMR are unknown, it is likely that EMR relies on the intrinsic properties of cartilage as a charged polymer hydrogel and the capacity for matrix constituents and extracellular electrolytes to participate in redox reactions. The application of an electric field to cartilage through metal electrodes initiates and maintains electrochemical reactions at the tissue–electrode interfaces with the diffusion of redox byproducts along the electrical potential and chemical concentration gradients further throughout the tissue volume. Previously, we have demonstrated the dependence of the degree of shape change on applied voltage (electric field) and application time using simple flat plate surface electrodes [12]. Later studies identified a correlation between the degree of shape change and total charge transfer, suggesting that the basis for EMR is *in situ* redox chemistry [13]. The bend angle of cartilage samples subjected to surface electrode-based EMR in a semicylindrical jig increased with applied voltage (electric field) and application time [12], [13]. Total charge transfer increased with increasing voltage (electric field) due to an increase in the amplitude of electric current or with an increase in application time due to more current flow through the specimen [13].

We selected a needle geometry that would be relatively easy to implement and translate into a clinical setting while still providing significant reshaping. Needle electrodes should be spaced close enough (<10 mm) to reduce electrical resistance (and hence resistive heating), but far enough away from one another (>0.5 mm) to allow easy placement by surgeons. Notably, the insertion of these thin needle electrodes (0.3 mm in diameter) causes little mechanical trauma to tissue within the region of the bend where internal stress is increased. In a previous study, we have found that needle electrodes do not produce any damage to cartilage apart from mechanical perforation [14]. No damage to chondrocytes was detected on subsequent live–dead staining.

Rabbit nasal septal cartilage served as the tissue model for this study. In addition to having extensive experience working with this tissue model [18]–[25], there are several reasons for our choice. First, rabbit septal cartilage has a similar function and microscopic structure compared to human hyaline cartilage, and is thus a representative model for translation to clinical use in human subjects [26]. Second, rabbit septal cartilage is relatively uniform among different animals [11]. Third, rabbit crania are readily available in bulk quantities and the septum is easy to extract, making it a practical choice for detailed systematic experiments that map a dosimetry parameter space such as in this study.

The finite element model, which is helpful, has obvious limitations. First, it is only able to estimate initial electric field prior to the onset of EMR. In practice, the electric field continually changes as redox reactions evolve in tissue. Second, though our results reconfirm the relationship between electric field and reshaping, the electric field range

selected for needle-based EMR studies was ultimately approximated using data obtained from surface electrode EMR studies. Yet there are marked similarities in electric field distribution between the two jig models. Specifically, the simulated profile of the electric field within the semicylindrical jig varies within approximately 10% between convex to concave electrodes and does not depend on the applied voltage amplitude [Fig. 2(b) and (c)]. In contrast, the peak field strength at the needle electrode–cartilage interface is approximately three times higher than in the central region of the sample along the bend axis [profiles B1–B1 and B3– B3 in Fig. 3(d), respectively]. However, the field within the 90° bend sector [profiles A3–A3 and B3–B3 in Fig. 3(c) and (d), respectively] is more uniform —with approximately 50% variation—making it possible to draw rough comparisons between the semicylindrical and 90° jigs. Third, unlike surface electrode EMR, there is currently a very limited understanding of the effect of needle-based EMR on chondrocyte viability. Intrinsic differences in size and traumatic effects between the two electrode types suggest potentially significant differences in the extent of tissue injury. Post-EMR tissue viability is beyond the scope of this work and further investigations are necessary to better define the relationship between electrical dosimetry, electric field distribution, shape change, and tissue viability. We again emphasize that this modeling effort is limited, but used at this juncture to reduce the expansive number of voltage, electrode geometry, and polarity combinations.

As expected, we observed a general increase in the reshaping angle with increase in applied voltage and application time (see Figs. 4 and 5). However, in contrast to previous observations of reshaping in a semicylindrical jig [12], [13] we did not detect a gradual increase in reshaping angle until a threshold value in voltage and application time was exceeded. Incremental increase in voltage did not result in corresponding increase in the reshaping angle above 19 ±2° of control value until voltages of 2, 6, and 4 V were applied in experiments lasting 1, 2, and 4 min, respectively (see Fig. 4). Similar to observations made with surface electrodes, control specimens demonstrated statistically significant “reshaping,” which is likely attributable to microfractures of the cartilage matrix following mechanical compression within the sharp bend leading to short-term shape maintenance.

The threshold effects observed in this study are inherently linked to the mechanism of EMR. For voltages below 2 V, the current in the EMR circuit was negative while it was positive above 2 V. Similar to experiments using the semicylindrical jig, in which negative current is observed below 1 V, it is likely that this change in current direction from negative to positive results in voltage- and time-dependent reduction reactions at the cathode and oxidation reactions at the anode [13]. This, in turn, generates electrochemical products in a selective space and produces changes in tissue biomechanics leading to long-term reshaping. It is speculated that there are numerous different chemical products yielded from different redox reactions which must act synergistically on the tissue before shape change can occur. The observed voltage threshold is thus likely a manifestation of increasing voltage causing increased reaction rates, which stimulates the accelerated formation of chemical products necessary to effect the shape change. Similarly, the observed application time threshold is likely due to the formation of chemical products as all reactions gradually proceed to completion over time. In each case, it is the point at which all chemical products are formed at adequate concentrations at the tissue–electrode interfaces that finally drives the shape

change at a threshold voltage and/or application time. Likewise, a threshold for the onset of the shape change may also exist for the semicylindrical EMR geometry, but was not detected due to low voltage resolution (1–2 V) of experimental studies [13].

The threshold voltage value does not appear to have a clear relationship with application time. While the mechanism of action for EMR is unknown, our assumption is that it is related to electrochemical changes in the tissue matrix macromolecules along with the hydrolysis of water and transient pH changes. The accumulation of species generated by redox reactions is not monotonous with time and voltage. At least two processes that determine the concentration of chemically active species are present: 1) direct production of electrochemically active species at the needle–electrode interface and 2) diffusion of these products to and from electrodes down both electrical and concentration gradients. We have confirmed that diffusion processes are dominant from 60 to 120 s application time [13]. The threshold voltage increases from 2 to 6 and then drops to 4 V as application time changes from 1 to 2 and 4 min, respectively. However, observed reshaping angles in the 2–4 V and 1–2 min range are statistically the same. Even though after 1 min of voltage application the reshaping angles observed at 2 and 4 V are statistically different from the angles observed at 0 and 1 V, application of 2 and 4 V for 1 and 2 min produce statistically similar reshaping angles. Thus, in future work, we will identify the threshold voltage values using dosimetry pairs of 6, 6, and 4 V for 1, 2, and 4 min of application time, respectively.

We believe that apparent irregularity in threshold voltage clearly demonstrates the complexity of the electrochemical reshaping process and should be taken into account in planning EMR procedures and reducing this technology to clinical practice. However, above the threshold voltage values, the reshaping angle fortunately increases in a predictable manner. Each incremental increase in voltage or application time produces statistically significant increase in the bend angle. In the previous studies we demonstrated a saturation effect in reshaping when further increase in applied voltage or application time does not produce significant increase in reshaping [12], [13]. The saturation effect may be explained by a threshold dosimetry set above which overwhelming tissue damage renders the tissue biomechanical properties indistinguishable from each other. In this study, the maximal voltage and application time (8 V, 4 min) is in the range of parameters known to be able to produce diffuse cartilage injury, but the saturation effect was not observed. The optimal voltage–time combinations for clinically relevant EMR should be found between reshaping onset and saturation thresholds.

V. Conclusion

This study demonstrated the potential clinical value of electromechanical cartilage reshaping using two arrays of needle electrodes located parallel to the line of a 90° bend in a rabbit nasal septal cartilage tissue model. Numerical model of electric field distribution within the reshaping jig was developed to guide electrode placement and select application voltage. The reshaping angle as a function of voltage and application time was systematically evaluated, with identification of a voltage threshold above which significant reshaping can occur. A significant variation in the reshaping angle obtained with voltages close to the threshold value was observed. However, above the threshold, the reshaping becomes regular

and predictable. Despite having limited information about chondrocyte viability at this point, EMR appears to produce clinically significant cartilage reshaping that is at par similar to conventional surgical techniques such as morselization and laser cartilage reshaping. Our findings may be used to guide clinical correction of cartilage deformations as well as create shape change in other tissues and biomaterials, once again attesting to the value of EMR as a minimally invasive, low cost, easy-to-implement treatment modality with numerous functional and aesthetic applications.

Acknowledgments

The authors would like to thank A. Lim for editorial assistance and assistance with experiments.

This work was supported by the Air Force Office of Scientific Research under Grant FA9550-04-1-0101, the Department of Defense Deployment Related Medical Research Program under Grant DR090349, and the National Institutes of Health under Grant DE019026, Grant DC005572, Grant DC00170, and Grant RR-01192.

References

1. Helidonis E, Sobol E, Kavvalos G, Bizakis J, Christodoulou P, Velegrakis G, Segas J, Bagratashvili V. Laser shaping of composite cartilage grafts. Am. J. Otolaryngol. 1993 Nov-Dec;14:410–412. [PubMed: 8285311]
2. Wang Z, Perrault DF Jr, Pankratov MM, Shapshay SM. Endoscopic laser-assisted reshaping of collapsed tracheal cartilage: a laboratory study. Ann. Otol. Rhinol. Laryngol. 1996 Mar.105:176–181. [PubMed: 8615580]
3. Wong BJ, Milner TE, Harrington A, Ro J, Dao X, Sobol EN, Nelson JS. Feedback-controlled laser-mediated cartilage reshaping. Arch. Facial Plast. Surg. 1999 Oct-Dec;1:282–287. [PubMed: 10937116]
4. Ovchinnikov Y, Sobol E, Svistushkin V, Shekhter A, Bagratashvili V, Sviridov A. Laser septochondrocorrection. Arch. Facial Plast. Surg. 2002 Jul-Sep;4:180–185. [PubMed: 12167077]
5. Trelles MA, Mordon SR. Correction of ear malformations by laser-assisted cartilage reshaping (LACR). Lasers Surg. Med. 2006 Aug.38:659–662. [PubMed: 16799999]
6. Keefe MW, Rasouli A, Telenkov SA, Karamzadeh AM, Milner TE, Crumley RL, Wong BJ. Radiofrequency cartilage reshaping: efficacy, biophysical measurements, and tissue viability. Arch. Facial Plast. Surg. 2003 Jan-Feb;5:46–52. [PubMed: 12533139]
7. Thomas L. Reversible collapse of rabbit ears after intravenous papain, and prevention of recurrence by prostone. J. Exp. Med. 1956; 104:245–252. [PubMed: 13345969]
8. Brent B. Auricular repair with autogenous rib cartilage grafts: Two decades of experience with 600 cases. Plast. Reconstr. Surg. 1992 Sep.90:355–374. discussion 375–376. [PubMed: 1513882]
9. Brent B. Technical advances in ear reconstruction with autogenous rib cartilage grafts: Personal experience with 1200 cases. Plast. Reconstr. Surg. 1999 Aug.104:319–334. discussion 335–338. [PubMed: 10654675]
10. Lovice DB, Mingrone MD, Toriumi DM. Grafts amd implants in rhinoplasty and nasal reconstruction. Otolaryngol. Clin. North Am. 1999 Feb.32:113–141. [PubMed: 10196441]
11. Wu EC, Khan A, Protsenko DE, Dubin S, Karimi K, Lim A, Shaikh MF, Li M, Wong BJ. Electromechanical reshaping of rabbit septal cartilage: A six needle-electrode geometric configuration. Proc. Soc. Photo. Opt. Instrum. Eng. 2009; 7161:716128-1–716128-11.
12. Ho KH, Diaz Valdes SH, Protsenko DE, Aguilar G, Wong BJ. Electromechanical reshaping of septal cartilage. Laryngoscope. 2003 Nov.113:1916–1921. [PubMed: 14603047]
13. Protsenko DE, Ho K, Wong BJ. Stress relaxation in porcine septal cartilage during electromechanical reshaping: mechanical and electrical responses. Ann. Biomed. Eng. 2006 Mar. 34:455–464. [PubMed: 16450186]

14. Manuel CT, Foulad A, Protsenko DE, Sepehr A, Wong BJ. Needle-electrode-based electromechanical reshaping of cartilage. Ann. Biomed. Eng. 2010 Jul.38:3389–3397. [PubMed: 20614240]
15. Protsenko DE, Ho K, Wong BJ. Survival of chondrocytes in rabbit septal cartilage after electromechanical reshaping. Ann. Biomed. Eng. 2010 Sep.39:150–156.
16. Cakmak O, Buyuklu F, Yilmaz Z, Sahin FI, Tarhan E, Ozluoglu LN. Viability of cultured human nasal septum chondrocytes after crushing. Arch. Facial Plast. Surg. 2005 Nov-Dec;7:406–409. [PubMed: 16301462]
17. Garg R, Shaikh M, Foulad A, Wong B. Chondrocyte viability in human nasal septum after morselization. Arch. Facial Plast. Surg. 2010 May-Jun;12:204–206. [PubMed: 20479439]
18. Chao KK, Ho KH, Wong BJ. Measurement of the elastic modulus of rabbit nasal septal cartilage during Nd:YAG (λ= 1.32 μm) laser irradiation. Lasers Surg. Med. 2003; 32:377–383. [PubMed: 12766960]
19. Karamzadeh AM, Chang JC, Diaz S, Milner T E, Wong BJ. Long-term *in vivo* stability of rabbit nasal septal cartilage following laser cartilage reshaping: A pilot investigation. Lasers Surg. Med. 2005 Feb.36:147–154. [PubMed: 15704163]
20. Wright R, Protsenko DE, Diaz S, Ho K, Wong B. Shape retention in porcine and rabbit nasal septal cartilage using saline bath immersion and Nd:YAG laser irradiation. Lasers Surg. Med. 2005 Sep. 37:201–209. [PubMed: 16127702]
21. Wong BJ, Pandhoh N, Truong MT, Diaz S, Chao K, Hou S, Gardiner D. Identification of chondrocyte proliferation following laser irradiation, thermal injury, and mechanical trauma. Lasers Surg. Med. 2005 Jul.37:89–96. [PubMed: 15900561]
22. Kaiser ML, Karam AM, Sepehr A, Wong H, Liaw LH, Vokes DE, Wong BJ. Cartilage regeneration in the rabbit nasal septum. Laryngoscope. 2006 Oct.116:1730–1734. [PubMed: 17003728]
23. Karam AM, Protsenko DE, Li C, Wright R, Liaw LH, Milner TE, Wong BJ. Long-term viability and mechanical behavior following laser cartilage reshaping. Arch. Facial Plast. Surg. 2006 Mar-Apr;8:105–116. [PubMed: 16549737]
24. Li C, Protsenko DE, Zemek A, Chae YS, Wong B. Analysis of Nd:YAG laser-mediated thermal damage in rabbit nasal septal cartilage. Lasers Surg. Med. 2007 Jun.39:451–457. [PubMed: 17565732]
25. Holden PK, Li C, Da Costa V, Sun CH, Bryant SV, Gardiner DM, Wong BJ. The effects of laser irradiation of cartilage on chondrocyte gene expression and the collagen matrix. Lasers Surg. Med. 2009 Sep.41:487–491. [PubMed: 19639619]
26. Wong BJ, Chao KK, Kim HK, Chu EA, Dao X, Gaon M, Sun CH, Nelson JS. The porcine and lagomorph septal cartilages: models for tissue engineering and morphologic cartilage research. Am. J. Rhinol. 2001 Mar-Apr;15:109–116. [PubMed: 11345149]

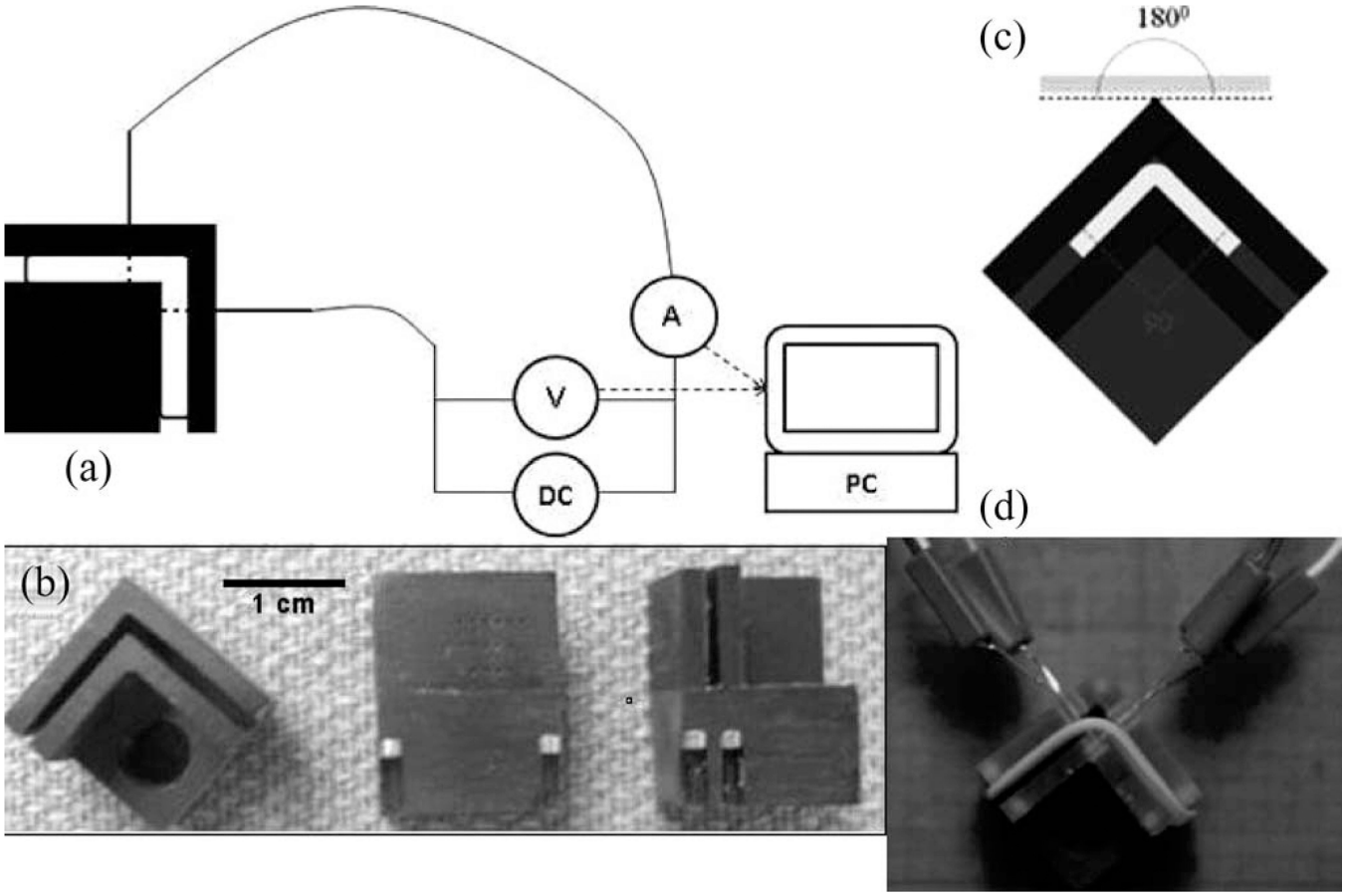

Figure 1.

(a) Schematic of needle-electrode-based EMR. Tissue specimen is secured within jig bent at 90° and electrode arrays are inserted bilaterally 3 mm from the bend axis. (b) Various views of custom precision-machined jig used in EMR experiments. (c) and (d) The tissue specimen is deformed to an initial bend angle of approximately 90° and secured in a precision-machined jig with insertion slots for platinum needle electrodes. During EMR, voltage (0, 1, 2, 4, 6, 8 V) is applied for a designated period of time (1, 2, 4 min), generating current through the needle electrodes into the cartilage tissue under mechanical stress.

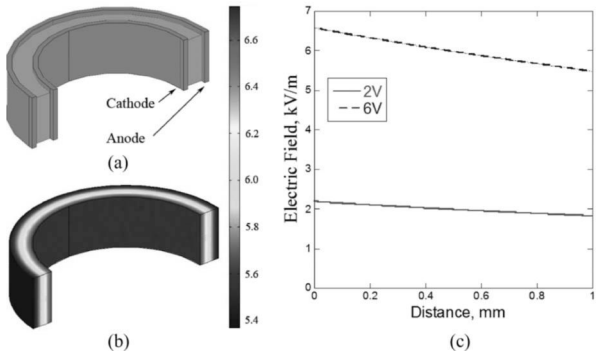

Figure 2.

(a) Cartilage specimen mounted between two semicylindrical electrodes. (b) Electric field distribution within the cartilage specimen. (c) Electric field from the cathode to anode electrode calculated for applied voltage of 8 V.

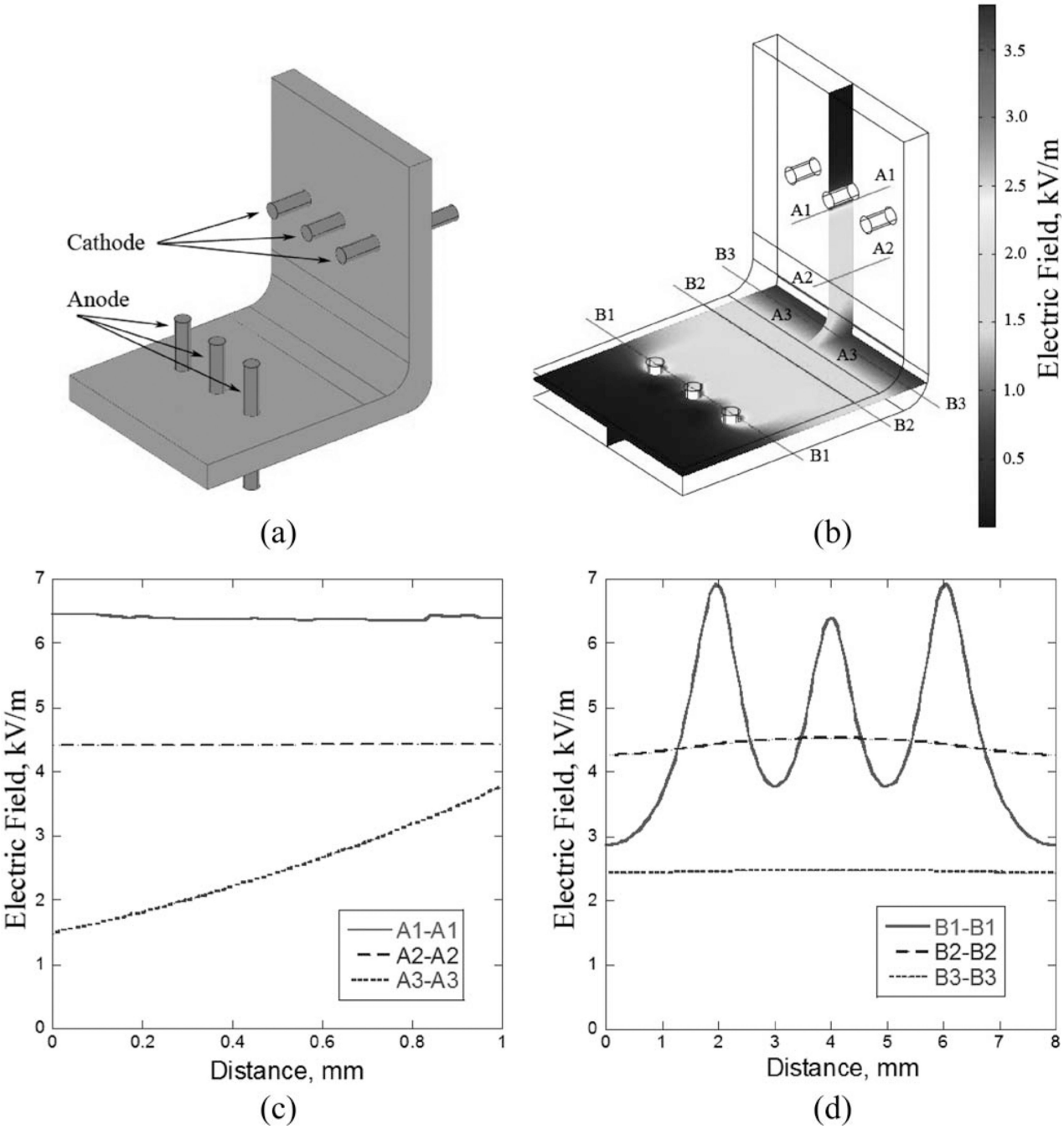

Figure 3.

(a) Cartilage sample bent into 90∞in a jig with six needle electrodes. (b) Electric field distribution within cartilage sample. (c) and (d) Electric field along cross sections as indicated in (b) calculated for applied voltage of 8 V.

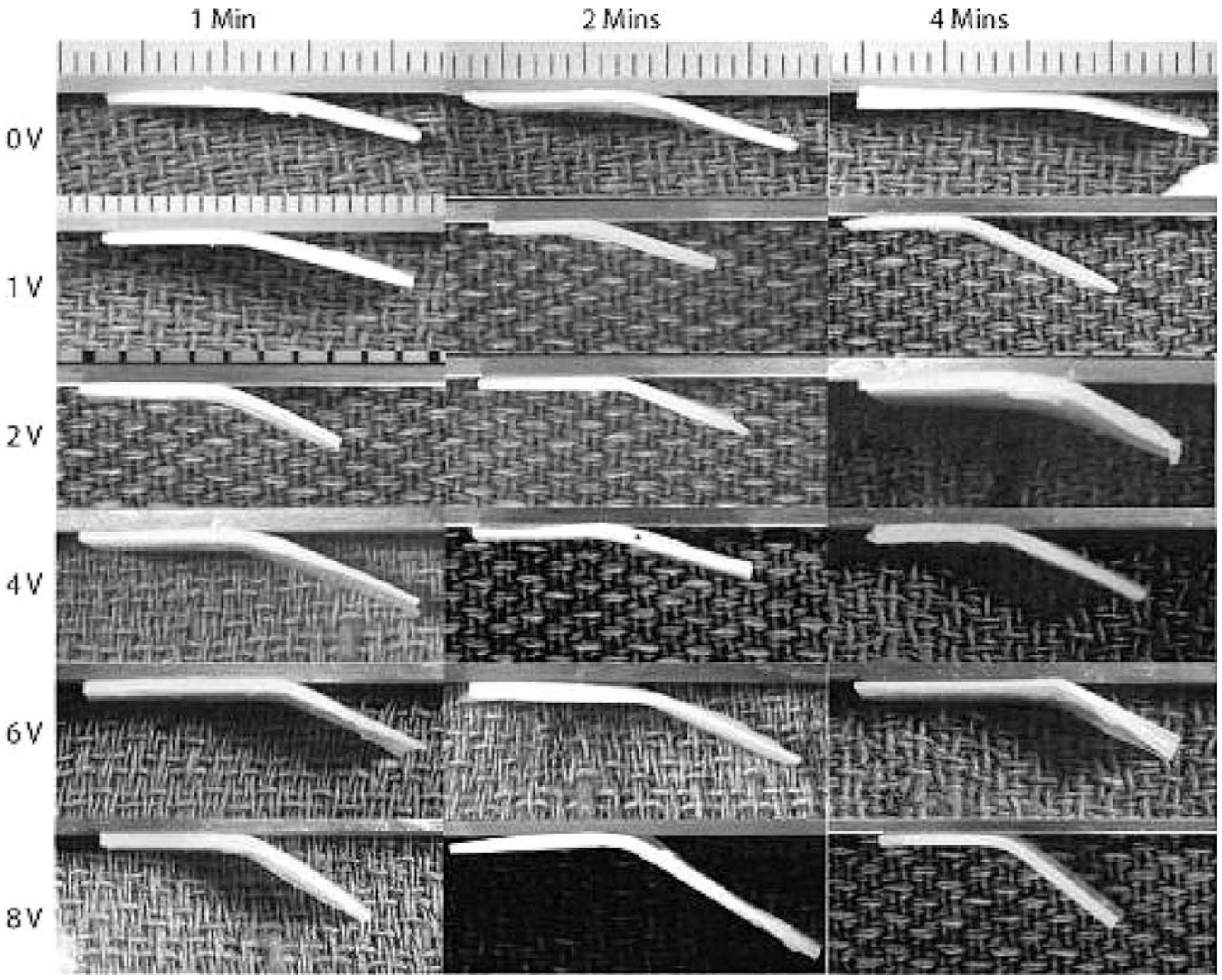

Figure 4.
Tissue specimens visibly showed significant differences in the bend angle as voltage and application time are varied.

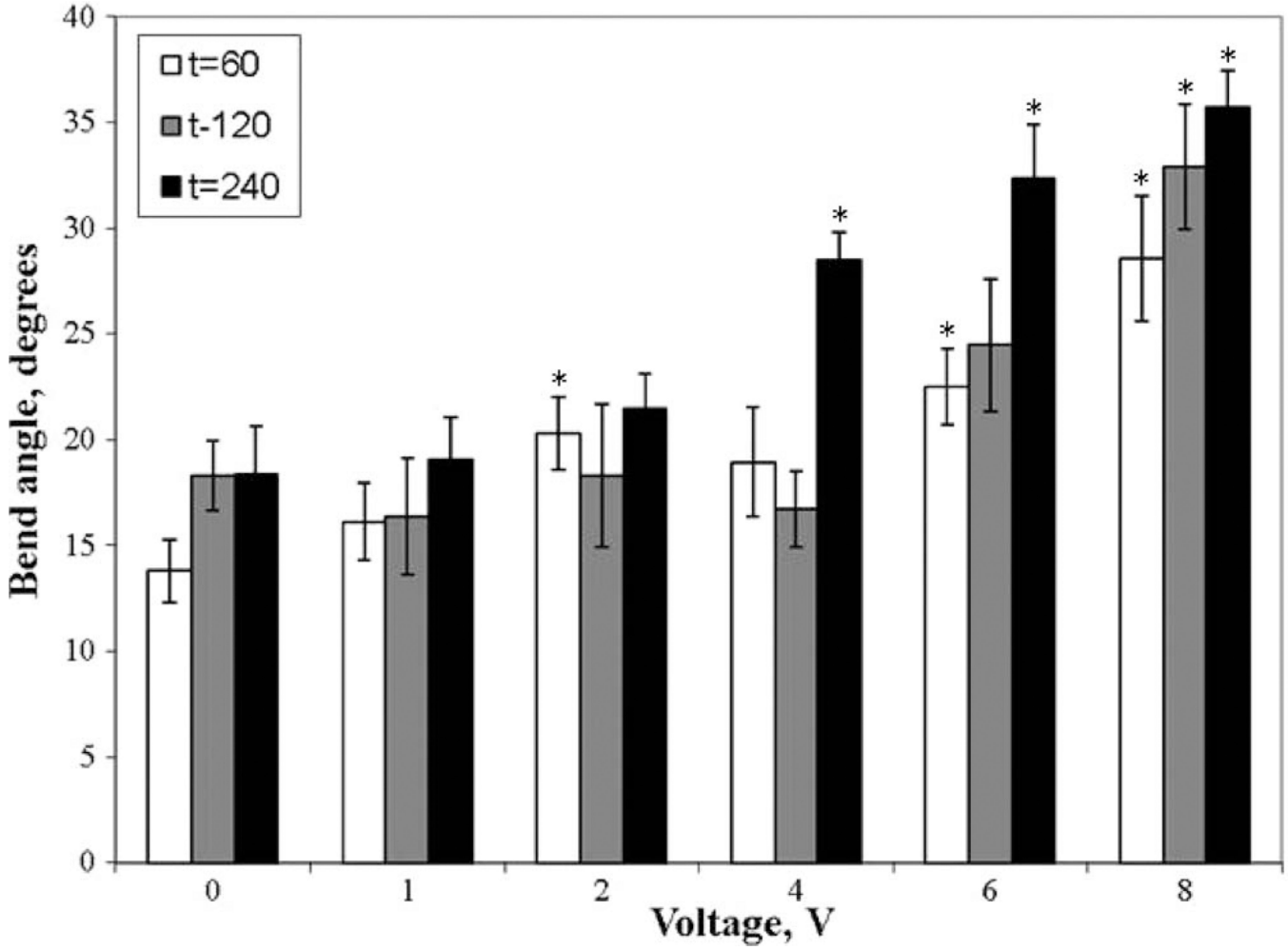

Figure 5.

Bend angle as a function of voltage with application times of 60 s (white bars), 120 s (gray bars), and 240 s (solid bars) (n = 7–15). Asterisks indicate statistically significant shape change ($\alpha < 0.05$) compared to controls under similar application times.

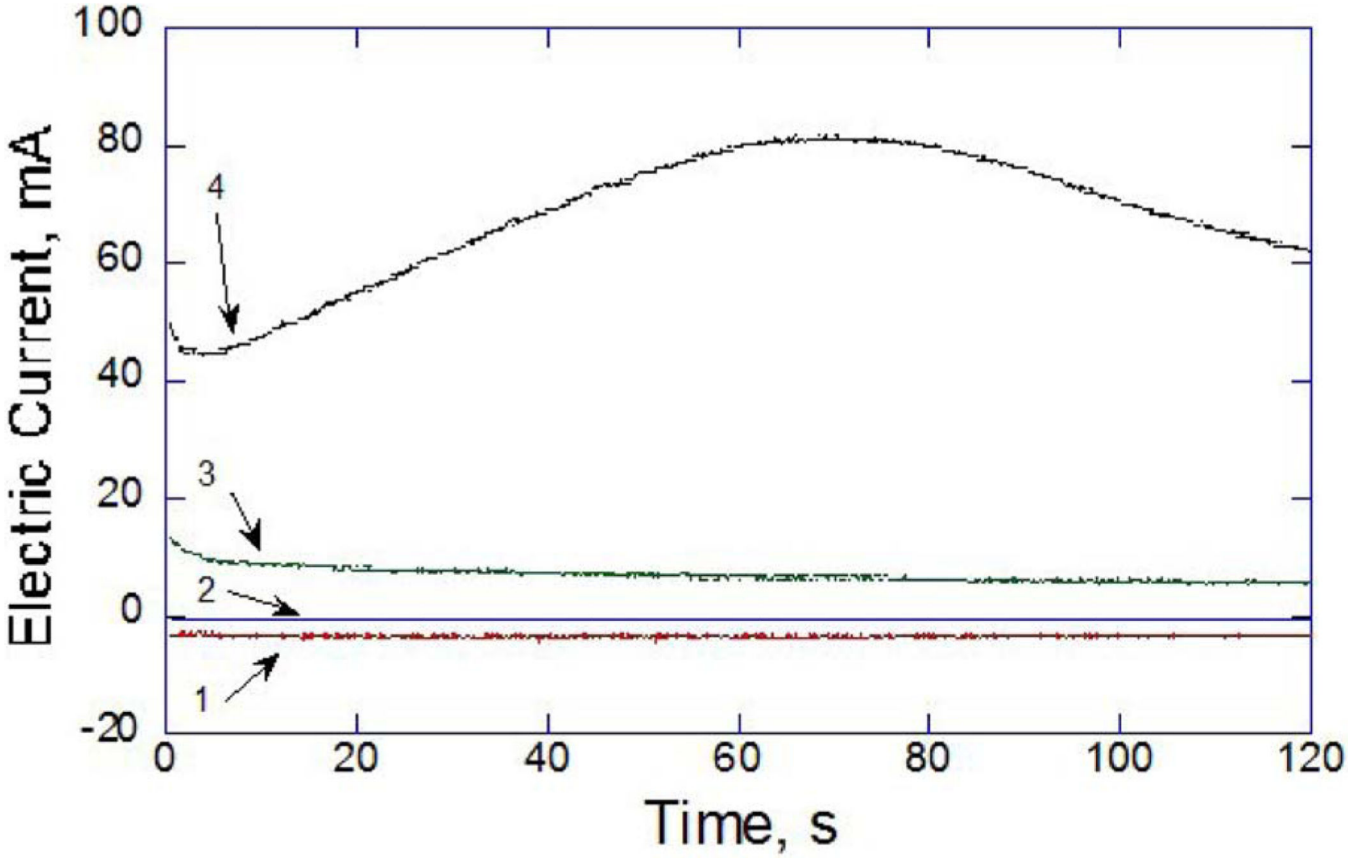

Figure 6.
Typical electric current during 2 min applications measured at (1) 0, (2) 2, (3) 4, and (4) 8 V.